Poly-L-Lactic Acid Nanofiber–Polyamidoamine Hydrogel Composites: Preparation, Properties, and Preliminary Evaluation as Scaffolds for Human Pluripotent Stem Cell Culturing

Chiara Gualandi, Nora Bloise, Nicolò Mauro, Paolo Ferruti, Amedea Manfredi, Maurilio Sampaolesi, Anna Liguori, Romolo Laurita, Matteo Gherardi, Vittorio Colombo, Livia Visai, Maria Letizia Focarete,* Elisabetta Ranucci*

Electrospun poly-L-lactic acid (PLLA) nanofiber mats carrying surface amine groups, previously introduced by nitrogen atmospheric pressure nonequilibrium plasma, are embedded into aqueous solutions of oligomeric acrylamide-end capped AGMA1, a biocompatible polyamidoamine with arg-gly-asp (RGD)-reminiscent repeating units. The resultant mixture is finally cured giving PLLA-AGMA1 hydrogel composites that absorb large amounts of water and, in the swollen state, are translucent, soft, and pliable, yet as strong as the parent PLLA mat. They do not split apart from each other when swollen in water and remain highly flexible and resistant, since the hydrogel portion is covalently grafted onto the PLLA nanofibers via the addition reaction of the surface amine groups to a part of the terminal acrylic double bonds of AGMA1 oligomers. Preliminary tested as scaffolds, the composites prove capable of maintaining short-term undifferentiated cultures of human pluripotent stem cells in feeder-free conditions.

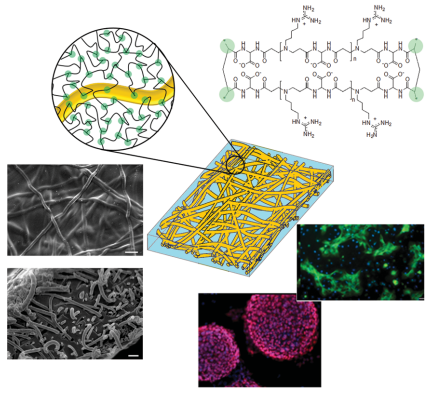

Dr. C. Gualandi, Prof. M. L. Focarete
Department of Chemistry "G. Ciamician" and INSTM UdR of Bologna
University of Bologna
40126 Bologna, Italy
E-mail: marialetizia.focarete@unibo.it
Dr. N. Bloise, Prof. L. Visai
Department of Molecular Medicine
Center for Health Technologies (CHT)
INSTM UdR of Pavia
University of Pavia
27100 Pavia, Italy
Dr. N. Mauro, Prof. P. Ferruti, Dr. A. Manfredi, Prof. E. Ranucci
Dipartimento di Chimica
Università degli Studi di Milano and INSTM – UdR Milano
20133 Milano, Italy
E-mail: elisabetta.ranucci@unimi.it
Dr. N. Mauro
Dipartimento di Scienze e Tecnologie Biologiche Chimiche e Farmaceutiche
University of Palermo
90128 Palermo, Italy
Prof. M. Sampaolesi
Interuniversity Institute of Myology and Department of Public Health
Experimental and Forensic Medicine
Division of Human Anatomy
University of Pavia
27100 Pavia, Italy
Prof. M. Sampaolesi
Translational Cardiomyology Laboratory
Department of Development and Regeneration
KUL University of Leuven
3000 Leuven, Belgium

Macromol. Biosci. **2016**, *16*, 1533–1544

DOI: 10.1002/mabi.201600061

1. Introduction

Polymeric hydrogels are hydrophilic polymer networks that swell, but do not dissolve in water. They constitute the fundamental components of many tissue engineering devices and controlled drug delivery systems.[1–4] Polyamidoamines (PAAs) are a family of biocompatible and biodegradable water-soluble polymers with a recognized potential for biotechnological applications, prepared by polyaddition of prim- and sec-amines to bisacrylamides.[5] Cross-linked PAAs usually absorb large amounts of water and form hydrogels in aqueous media. Hydrogels arising from biocompatible PAAs have constantly been found biocompatible and biodegradable to nontoxic products.[6–9] Different PAA hydrogels were tested as substrates for cell culturing, and found adhesive toward different cell types.[6–11] 4–Aminobutylguanidine (agmatine) and 2,2-bisacrylamidoacetic acid gave the water-soluble amphoteric PAA called AGMA1 whose repeating unit, as shown in Figure 1, is reminiscent of the arg-gly-asp (RGD) motif, identified as the fibronectin sequence mediating cell attachment. It had previously been demonstrated that modification with agmatine imparted poly(propylene fumarate-co-ethylene glycol) hydrogels enhanced fibroblast adhesion.[12] This was associated with the RGD-mimic structure of the guanidine side groups. Linear AGMA1 proved highly biocompatible.[13,14] In the form of thin film, it acted as excellent adhesion and proliferation promoter of primary neural cells such as microglia, hippocampal neurons, and astrocytes. Neurons differentiated axons and dendrites, and established functional synaptic contacts. Electrophysiological tests provided evidence of neuron spontaneous activity.[15]

Cross-linked AGMA1 absorbed large amounts of water forming hydrogels. Performing the cross-linking reactions in the appropriate moulds gave AGMA1-hydrogel tubular conduits that were implanted in rats after removing a 1 cm portion of sciatic nerve. In three months, the nerve was regenerated with good histological morphology and functional recovery, and the conduits were completely reabsorbed with no evidence of local inflammation.[8] However, AGMA1 hydrogels had poor

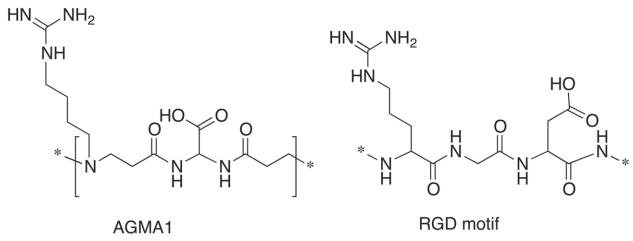

Figure 1. Chemical structures of AGMA1 repeating unit and RGD motif.

mechanical properties, and could not be fixed to the surrounding tissues by stitching, but only with fibrin glue. The radical polymerization of acrylamide-terminated AGMA1 oligomers in the presence of 2-hydroxyethylmethacrylate led to copolymeric hydrogels with somewhat improved mechanical properties.[16,17] Hydrogel/fiber composites, combining the advantages of both components, have a great potential as scaffolds for tissue engineering.[18–22] It was speculated that embedding biodegradable nanofibers in AGMA1 hydrogels would reinforce and make them suitable for in vivo tissue regeneration. Poly-L-lactic acid (PLLA) is a well-known biocompatible and biodegradable polyester universally accepted for human use as drug delivery system and prosthetic material.[23–25] It has excellent mechanical properties and is amenable to electrospinning.[26] PLLA nanofiber mats were, in principle, suitable reinforcements for AGMA1 hydrogels, but were incompatible with PLLA. It was speculated that covalently binding AGMA1 to PLLA nanofibers during the cross-linking step would overcome this problem. This was achieved by previously introducing surface amine groups on PLLA nanofibers with a treatment with nitrogen plasma. The synthetic strategy proved correct. The fibrous and matrix components of the resultant composites remained indefinitely anchored to each other even when fully swollen in water. It was previously reported that human pluripotent stem cells (hPSCs) cultured on hydrogels with optimal elasticity maintained their pluripotency for many passages.[27–29] Short time preliminary was carried out on the composites to explore their potential as scaffolds for hPSCs

A. Liguori, R. Laurita, M. Gherardi, V. Colombo
Department of Industrial Engineering (DIN) and Advanced Mechanics and Materials – Interdepartmental Center
University of Bologna
40131 Bologna, Italy
Prof. L. Visai
Laboratory of Nanotechnology
Department of Occupational Medicine
Toxicology and Environmental Risks
Salvatore Maugeri Foundation
IRCCS, Pavia, Italy

Prof. M. L. Focarete
Health Sciences and Technologies – Interdepartmental Center for Industrial Research (HST-ICIR)
University of Bologna
40064 Ozzano dell'Emilia, Italy

culturing, with favorable results. The aim of this paper is to report on these issues.

2. Experimental Section

2.1. Preparation of Hydrogel Composite Scaffolds and Corresponding Plain Hydrogels

Hydrogel composite scaffolds and plain hydrogels were prepared in the form of sheets using as mold two silanized glass plates of size 10 cm × 10 cm × 0.2 cm. The glass plates were rendered nonadhesive by soaking for 5 h in aqua regia at room temperature, then washing several times with water, drying, and exposing to chlorotrimethylsilane vapors for 3 d in a closed chamber. The plates were then soaked in toluene (20 mL), ethanol (2 × 20 mL), and water (3 × 20 mL) and finally gently wiped with soft paper and used immediately in the next steps.

2.1.1. Preparation of Composites Comp-10 and Comp-20

4,4′-Azobis(4-cyanovaleric) acid (25 mg) in water (0.5 mL) was added, respectively, to 40% (w/v) pH 5.0 aqueous solutions (2.5 mL) of AGMA1-10 or AGMA1-20 oligomers, prepared as previously reported[8] from 4-aminobutylguanidine/2,2-bisacrylamidoacetic acid with, respectively, 10% and 20% mol/mol excess bisacrylamide (Figure 2) (see Supporting Information for experimental details). The mixtures were stirred 1 min, then retrieved with a syringe and spread over the PLLA mat, which was gently pressed between the glass plates and exposed 10 min to UV irradiation (250 W lamp at 0.25 m distance). The composite samples were gently detached from the glass plates, and first soaked 4 h in water (2 × 200 mL), then in 0.1 × 10^{-3} M phosphate-buffered saline (PBS) pH 7.0 (1 × 200 mL).

2.1.2. Preparation of Plain Hydrogels HG-AGMA1-10 and HG-AGMA1-20

HG-AGMA1-10 and HG-AGMA1-20 were prepared by the same procedure but omitting Fiber-PLLA, using a 0.7 mm thick silicon spacer, and injecting the oligomer solutions in the mold with a syringe. The resultant hydrogels were retrieved and soaked as in the previous case, taking care of their superior fragility. Both composites and hydrogels were stored in 50% ethanol at 4 °C before use.

2.2. Characterization Methods

X-ray photoelectron spectroscopy (XPS) analyses were performed by means of a Specs PHOIBOS HSA 3500 instrument using nonmonochromatic Mg K_a radiation (13.5 kV, 20 mA). XPS spectra were acquired at 45° emission angle and normal to the sample surface. Surveys were acquired at 40 eV pass energy, step 1.0 eV while narrow scans at 20 eV pass energy and 0.1 step size. Binding energies were referenced to the C-H level at 285.0 eV.[30]

Water contact angle measurements were performed on Fiber-PLLA before and after plasma treatment using a KSV CAM101 instrument at ambient conditions. The side profiles of deionized water drops were recorded for image analysis. The shape of the drop was recorded in a time range of 0–30 s, collecting images every 1 s. At least ten drops were observed for each sample.

Sample morphology was investigated observing dried samples with a Philips 515 scanning electron microscope (SEM) at 15 kV accelerating voltage. Prior to SEM analysis, samples were sputter-coated with gold. Fiber diameter distributions were evaluated as the average of about 150 fibers using an image acquisition software (EDAX Genesis). The results were reported as the mean ± standard deviation (SD).

Swelling experiments were performed in ethanol, water, and PBS at pH 7.4 (prepared using Sigma-Aldrich tablets according to manufacturer's instructions) on 1 mm thick hydrogel discs with an 18 mm base diameter. Samples were dried to constant weight at 25 °C and 0.1 Tor before undergoing swelling. Each disc was put into a test tube containing 40 mL of the swelling medium and maintained at 25 °C. At regular intervals the disc was retrieved, gently wiped with soft filter paper, weighed, and reintroduced into the test tube. Maximum swelling was observed after about 1 h. The swelling extent, SW%, was determined using the following equation

$$SW\% = \frac{W_t - W_o}{W_o} \times 100$$

where W_0 is the weight of the dry disc and W_t is that of the fully swollen disc. The reported values were the average of six experiments. The percent mean variation coefficient, CV%, was always lower than 5%. Degradation was monitored measuring the weight loss of hydrogel samples maintained at 37 °C in pH 7.4 PBS for prolonged time. The percent weight loss, W_l%, was calculated according to the equation

$$W_l\% = \frac{W_o - W_{td}}{W_o} \times 100$$

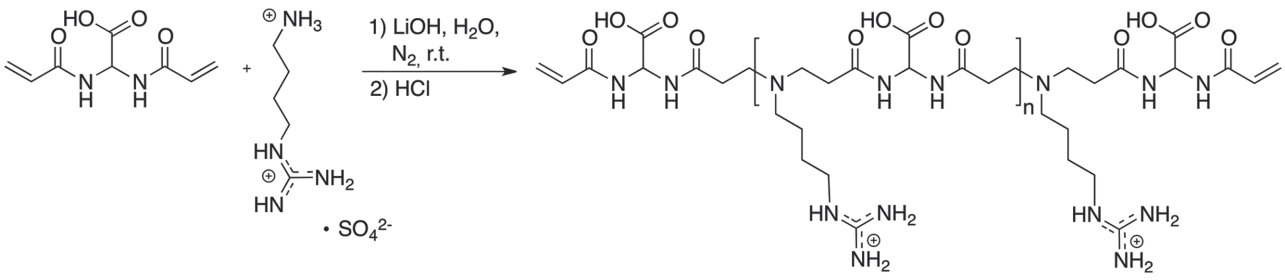

Figure 2. Synthesis of AGMA1-10 and AGMA1-20 oligomers.

where W_0 is the weight of the dry disc at initial time and W_{td} is the weight of the dried disc at t time. All experiments were performed in triplicate. The mean CV% was always lower than 5%. Stress–strain measurements were carried out using an Instron 4465 tensile testing machine on rectangular sheets 5 mm in width, with 20 mm gauge length. The thickness, measured by a microcaliper, was 25, 400–450, and 250–300 μm for fiber-PLLA, plain hydrogels, and composites, respectively. The cross-head speed was 5 mm min^{-1}. Plain hydrogels (HG-AGMA1-10 and HG-AGMA1-20) and composites (Comp-10 and Comp-20) were analyzed after having been swollen in water for 24 h. Fiber-PLLA was analyzed in the dried state. At least six replicate specimens were run for each sample, and results were provided as the average value ± SD. The one-way ANOVA was used to test the significance in the difference between the mean values ($p < 0.05$).

2.3. Cell Proliferation Assessment

The in vitro biological studies were performed on human embryonic stem cells (hESCs) (H9 ESCs, WiCell, Research Institute, Madison, WI) and human induced pluripotent stem cells (hiPSCs) (piPSC line, SBI System BioSciences, Mountain View, CA). Both hPSCs were maintained under feeder-free condition on plates coated with Matrigel (BD Biosciences, CA, USA) according to manufacturer instructions in mTeSR1 medium (Stem Cell Technologies, Vancouver, BC, Canada).[31] Cells were grown in 5% CO_2 at 95% relative humidity and passaged every 5–7 d with daily medium changes. Before cell seeding, hydrogels and composites were prepared for cell culture first by PBS washes and after by sterilization overnight under UV light. PLLA nanofibrous scaffolds were sterilized with a decreasing gradient of ethanol, followed by PBS washes before UV treatment for overnight. After sterilization, all the scaffolds were then placed into individual wells of 24-well plates, and rinsed three times with PBS before cell seeding. Unlike to the Tissue Culture Plates (TCPS), the scaffolds were not treated with conventional coatings (i.e., fibronectin, laminin, Matrigel) before cell plating. In brief, according to literature,[32] 10×10^{-6} M rho associated protein kinase (ROCK) inhibitor Y-27632 (Calbiochem, VWR, Belgium) was added to the cell cultures for 1 h at 37 °C before detaching of cells. After trypsinization, cells were re-suspended in culture medium and centrifuged at 1200 rpm for 5 min; the pellet was fully dispersed in mTeSR1 medium containing 10×10^{-6} M Rock Inhibitor Y-27632 and counted by trypan blue solution. The hESCs and hiPSCs were then seeded at a density of 1×10^5 cells cm^{-2} on the top of no-coated scaffolds in mTeSR1 medium containing 10×10^{-6} M Rock Inhibitor Y-27632 (Calbiochem, VWR, Belgium) and finally incubated at 37 °C in a humidified 5% CO_2, 95% air atmosphere incubator. Cells cultured on Matrigel-coated Tissue Culture Plates (TCPS-Mg) were used as positive control.

After 24 h from seeding, the medium was replaced with Y-27632 free mTeSR1, and then changed daily for all experiments. Cells cultured on Matrigel-coated Tissue Culture Plates (TCPS-Mg) were used as positive control. At days 1 and 7, the proliferation was assessed by the quantitative 3-[4,5-dimethylthiazol-2-yl]-2,5-diphenyl tetrazolium bromide (MTT) test (Sigma-Aldrich). Briefly, at each time, hPSCs-seeded scaffolds were transferred into a 24-well culture and the medium was replaced by 500 μL of DMEM medium, followed by the addition of 50 μL MTT (5 mg mL^{-1}).[33] The scaffolds were then incubated for 4 h at 37 °C in a humidified 5% CO_2 incubator. The formazan crystals, formed by the interaction of the MTT solution with the live cells, were then dissolved in a 1:1 v/v isopropanol-0.04 M HCl. Aliquots of 100 μL were sampled and the absorbance was measured at 570 nm by a microplate reader (BioRad Laboratories, Hercules, CA, USA).

2.4. Immunofluorescence

hPSCs-seeded scaffolds were prepared for indirect immunofluorescence to evaluate cell morphology and pluripotency. Briefly, the samples were washed with PBS and fixed 10 min at room temperature with a 4% (w/v) paraformaldehyde solution. Subsequently, the fixed cells were permeabilized with 0.2% Triton X-100 in 1% BSA, and blocked with 5% Donkey Normal Serum (Sigma-Aldrich, St Louis, MO, USA) for 1 h at room temperature. For morphological observation, hPSCs-seeded scaffolds sampled at 1 d of culture were incubated overnight at 4 °C in humid atmosphere with primary mouse antibody anti-β tubulin (Millipore, Billerica, MA, USA). After washing with PBS, samples were incubated 1 h at room temperature with Alexa Fluor 488 secondary antibodies (1:1000 in PBS, Invitrogen). For pluripotency factor labeling, hPSCs-seeded scaffolds sampled at 7 d of culture were incubated overnight at 4 °C in humid atmosphere with primary goat antibody anti-octamer-binding transcription factor 4 (OCT4, Santa Cruz, Dallas, TX, USA) diluted in permeabilization buffer (1:1000). Human skin fibroblasts were used as negative controls for OCT4. After washing with PBS, samples were incubated 1 h at room temperature with Alexa Fluor 594-conjugated secondary antibodies (1:1000 in PBS, Invitrogen). In all studies, parallel no primary antibody negative controls were undertaken. For both types of evaluations, after extensive washes with PBS, hPSCs-scaffolds were incubated with Hoechst 33342 for nuclei staining (diluted 1:1000 in PBS). Images were acquired using an Eclipse TS100 microscope (Nikon, Japan).

2.5. Gene Expression Analysis

For gene expression analysis, total RNA was extracted from cultured hPSCs using the PureLink RNA Mini Kit (Life Technologies, Carlsbad, CA, USA) according to the manufacturer's instructions, including treatment with RNase free DNase to remove genomic DNA (TURBO DNA-Free Kit, Life Technologies). RNA was quantified and retro-transcribed to cDNA using the Superscript III Reverse Transcriptase Kit (Life Technologies). For quantitative (q) RT-PCR analysis, Fast SYBR Green Master Mix (Life Technologies) was diluted with cDNA and primers and quantitative reverse transcription-PCR (qRT-PCR) was carried out using ViiA7 Real-Time PCR Real-Time PCR instrument (Applied Biosystems). Gene expression was analyzed in triplicate and normalized to glyceraldehyde 3-phosphate dehydrogenase (GAPDH) gene expression. Graphs represent means ± SD. The sequences of all primers employed in this study are shown in Table 1. For statistical analysis, differences between groups were tested by one-way ANOVA. Tukey's test was used to correct for multiple comparisons.

Table 1. Primers used for qRT-PCR.

Genes	Forward 5′-3′	Reverse 3′-5′	Amplicon size [bp]
GAPDH[a)]	GAAGGTGAAGGTCG-GAGTC	GAAGATGGT-GATGGGATTTC	225
NANOG[b)]	CATGAGTGTGGATC-CAGCTTG	CCTGAATAAGCAGATC-CATGG	191
OCT4[c)]	AGTGAGAGGCAACCTG-GAGA	ACACTCGGACCACATCCTTC	110
SOX2[d)]	TGGACAGTTACGCGCACAT	CGAGTAGGACATGCTG-TAGGT	215

[a)]GAPDH, glyceraldehyde-3-phosphate dehydrogenase; [b)]NANOG, Nanog Homeobox; [c)]OCT4, octamer-binding transcription factor 4; [d)]SOX2, SRY (sex determining region Y)-box 2.

Statistical significance was established at two-tailed $p \leq 0.05$. All calculations were generated using GraphPad Prism 5.0 (GraphPad Inc., San Diego, CA).

2.6. Cytotoxicity Evaluation of the Hydrogel Degradation Products

Both hydrogels and composite samples were incubated in DMEM (Life Technologies) at 37 °C, 5% CO_2 for 7 d. At the end of the degradation experiments, both pluripotent stem cells lines were exposed 24 h to DMEM containing the degradation products undiluted or diluted 1:2 and 1:4 in complete culture medium.

3. Results and Discussion

3.1. Rationale

The rationale of this work was to prepare PLLA/AGMA1 composites combining the biomimetic properties and softness of the surface-exposed AGMA1 hydrogel with the strength of PLLA mats. Both components are biodegradable, albeit at a faster rate for AGMA1, biocompatible and endowed with cell adhesiveness. These composites were designed adopting as benchmark the overall structure of tissue extracellular matrix (ECM). The scaffolds consisted of differently cross-linked AGMA1 hydrogels with embedded PLLA mats of 570 ± 170 nm diameter continuous electrospun nanofibers, mimicking the gel and fibrous components of ECM, respectively.

3.2. Composite Preparation

The composite preparation encompassed five steps. The first step was preparing highly porous electrospun PLLA nonwoven mats, named Fiber-PLLA (see SEM images in Figure 3A,B), according to a previously described procedure.[34,35]

The second step was preparing acrylamide end-capped AGMA1 oligomers amenable to be crosslinked by radical polymerization. In bifunctional stepwise polymerizations, the products of stoichiometrically unbalanced recipes have reduced molecular weight, and are end-capped with the excess function. Accordingly, the acrylamide end-capped oligomers were prepared by introducing excess bisacrylamide in the polymerization recipes as previously described.[5] In the present study, two acrylamide-end-capped oligomers named AGMA1-10 and AGMA1-20

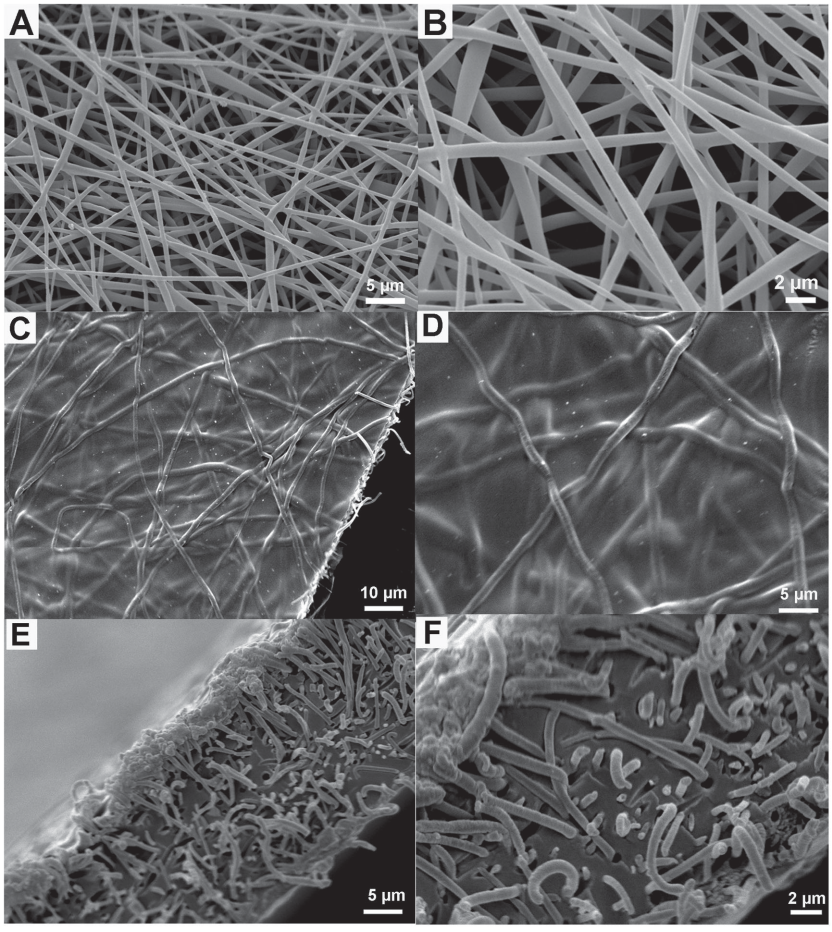

Figure 3. SEM images at different magnifications: A,B) Fiber-PLLA. C,D) Comp-10 top view. E,F) Comp-10 transverse section view.

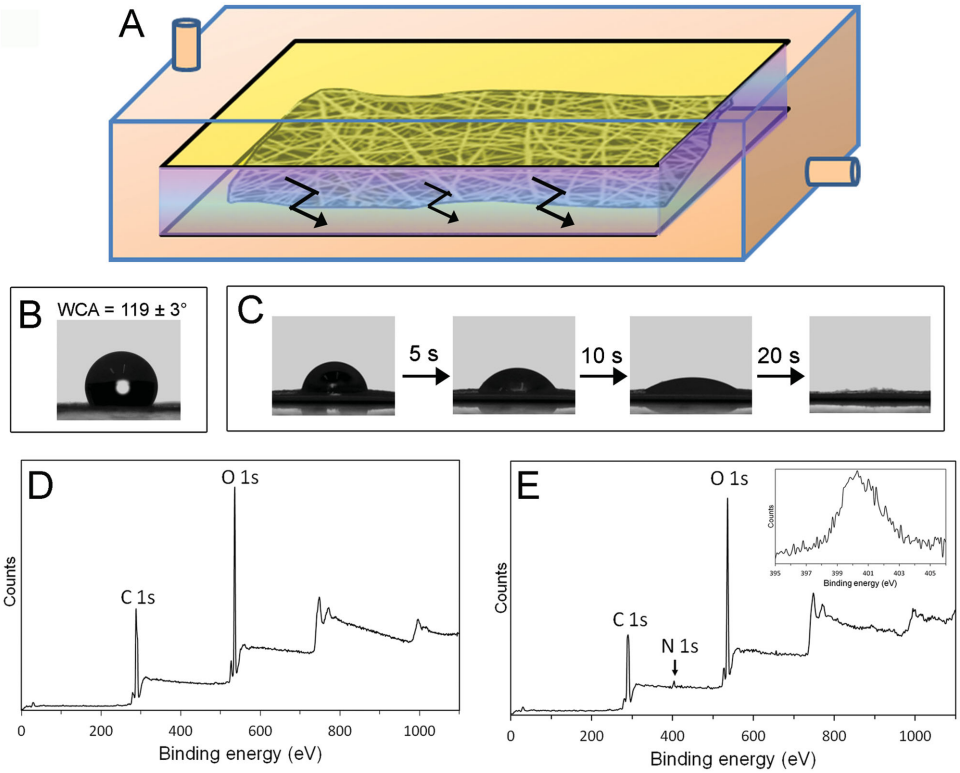

Figure 4. A) Sketch of Fiber-PLLA plasma treatment. B) Water droplet on as-spun Fiber-PLLA. C) Water droplet on Fiber-PLLA after nitrogen-plasma. D) XPS spectra of as-spun Fiber-PLLA. E) XPS spectra of Fiber-PLLA after nitrogen-plasma (narrow scan of N1s in the inset).

were prepared adopting recipes with 10- and 20 mol% excess bisacrylamides, respectively. The oligomers were obtained as 30% (w/v) aqueous solutions brought to pH 5–5.5 with hydrochloric acid before further processing.

As prepared, the mats did not absorb water (see later Figure 4B), likely due to the combination of intrinsic hydrophobicity and thinly porous structure.[35–37] This biased impregnation with the aqueous acrylamide-end-capped AGMA1 solutions. Accordingly, the third step consisted of treating the mats with nitrogen atmospheric-pressure plasma (see experimental details in the Supporting Information) (Figure 4A) in order to introduce surface amine groups (compare XPS spectra of Figure 4D,E). This treatment rendered the mats both hydrophilic, hence impregnable with the oligomer solutions (Figure 4C), and capable of covalently grafting a part of the AGMA1 oligomers by reacting with the terminal acrylamide groups. A similar surface conditioning had been previously adopted for stably binding different PAAs to poly(lactic-*co*-glycolic acid) films.[38]

The fourth step consisted of impregnating plasma treated Fiber-PLLA (Figure 5A), positioned between two silanized glass plates (Figure 5C,D), with the above aqueous acrylamide-end-capped AGMA1 solutions added of 4,4′-azobis(4-cyanovaleric acid) (5 wt% based on PAA) as radical initiator (Figure 5B).

The fifth and final step was curing, accomplished by triggering the radical polymerization of the residual acrylamide end groups by UV irradiation at room temperature.

The resultant hydrogels were firmly attached to the mat by the covalent bonds established with a part of the AGMA1 oligomeric precursors. Gently detaching from the glass plates, and extensively washing with MilliQ water and 0.1×10^{-3} M PBS pH 7.0 finally yielded transparent, soft, elastic, and macroscopically homogeneous AGMA1-based hydrogels with embedded Fiber-PLLA (Figure 5E,F). These composites were labeled Comp-10 and Comp-20 when obtained from AGMA1-10 and AGMA1-20, respectively. Their SEM images in the dry state (Figure 3C–F for Comp-10 and S4 for Comp-20) show that the hydrogel matrix completely filled the mat pores and that PLLA fibers were evenly distributed underneath the composite surface, preserving the original texture.

3.3. Plain AGMA1 Hydrogels

For comparison purposes, plain AGMA1 hydrogels, henceforth referred to as HG-AGMA1-10 and HG-AGMA1-20, were prepared by radical polymerization of the acrylamide-terminated AGMA1 oligomers under the same curing conditions of the corresponding composites, but in the absence of PLLA mats.

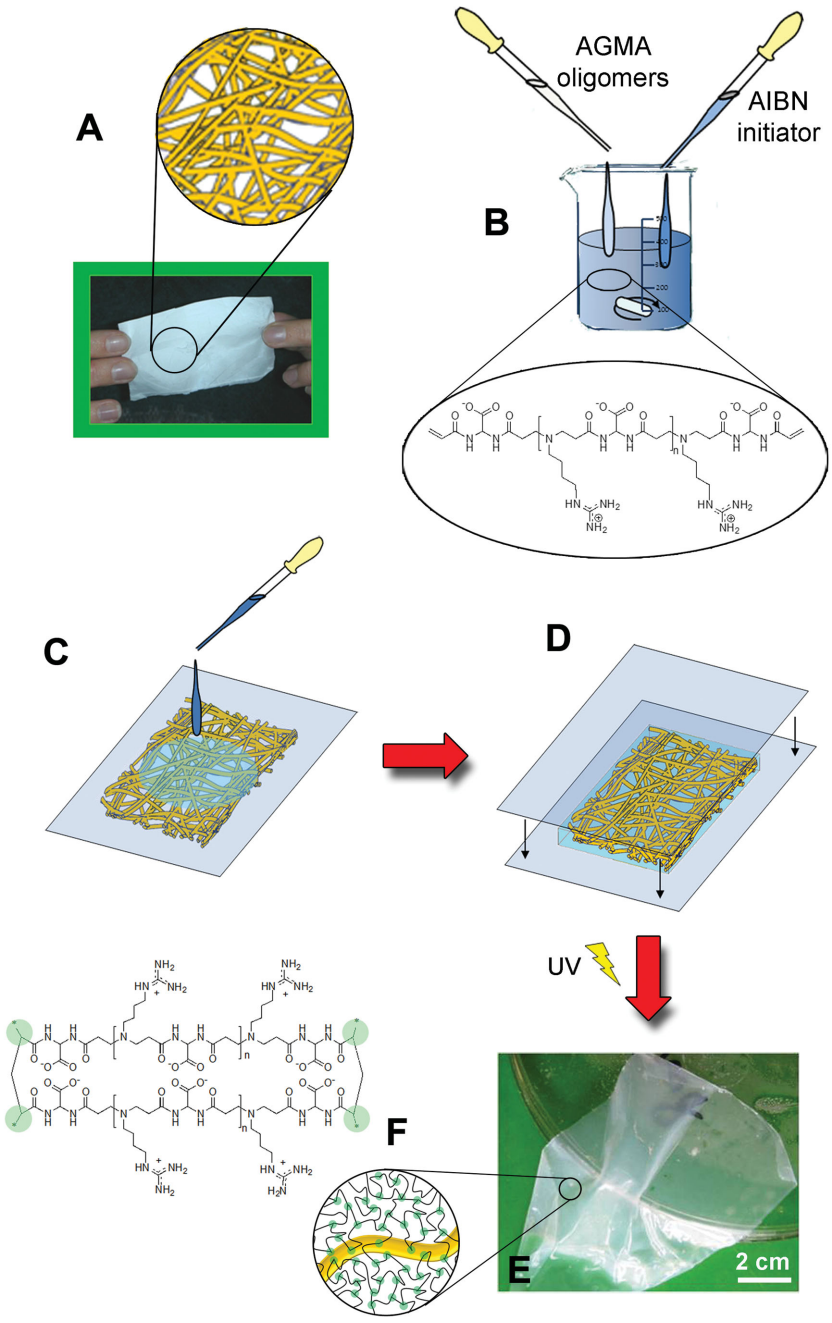

Figure 5. Comp-10 and Comp-20 preparation steps. A) Macroscopic aspect of Fiber-PLLA and sketch of nonwoven fibers. B) AGMA1 oligomers impregnating solution. C) Impregnation of N_2-plasma treated Fiber-PLLA mats. D) Interposition of the impregnated mats between two glass sheets. E) Macroscopic aspect of the final products fully water-swollen. F) Sketch of nonwoven fibers embedded in a hydrogel AGMA1 cross-linked matrix.

3.4. Swelling and Degradation Behavior

Comp-10 and Comp-20 swelled in aqueous media neither breaking nor splitting apart and remained highly flexible and resistant, confirming the good interfacial fiber/hydrogel adhesion, hence the efficacy of the fiber/matrix immobilization. It may be observed that if the nitrogen plasma treatment was omitted, that is, in the absence of chemical grafting, in the resultant composites hydrogel and fibers detached from each other and the structure collapsed within 2–3 h swelling in water. As regards the hydrogels, water-swollen HG-AGMA1-10 and HG-AGMA1-20 were transparent and flexible, but very fragile and difficult to handle.

Figure 6 compares Comp-10 and Comp-20 swelling ability with that of HG-AGMA1-10 and HG-AGMA1-20 in PBS or DMEM buffers, characterized by different ionic strength, after 24 h. The swelling degree of Comp-10 was dramatically lower than Comp-20, whereas HG-AGMA1-20 swelled only slightly less than HG-AGMA1-10. These data are apparently conflicting, but it should be noticed that the precursor of Comp-20 has approximately twice as many double bonds than Comp-10. Therefore, in the crosslinking step it is liable to form many more covalent bonds with the PLLA fibers, rendering the composite more tightly interconnected, hence less swellable than expected from the corresponding plain hydrogels.

Degradation tests were performed on composites and plain hydrogels by monitoring the percent weight loss after 3 and 7 d at 37 °C in DMEM buffer pH 7.4 (Figure 7). The extent of cross-linking significantly affected the hydrogel degradation rate, the more cross-linked samples degrading slower. By contrast, the difference between composites and their plain hydrogel counterparts was modest, since under the conditions adopted the PLLA fibers degraded at a significantly lower rate, and the composite weight loss was to be ascribed solely to their hydrogel component. This was not unexpected, since it had been previously demonstrated that AGMA1 hydrogels were completely degraded in vivo within 3 months,[7] whereas PLLA is known to degrade much slowly and to maintain its physical integrity for several months.

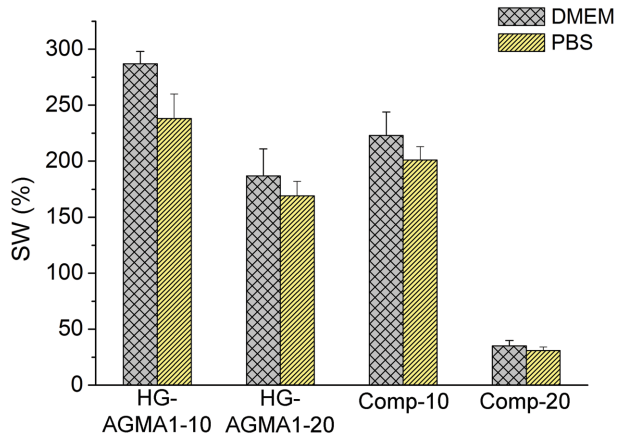

Figure 6. Swelling degree after 1 d immersion in DMEM and PBS.

3.5. Tensile Stress–Strain Tests

The results of tensile stress–strain tests performed on both plain hydrogels and composites are reported in Figure 8. As regards hydrogels, HG-AGMA1-10 exhibited lower elastic modulus, E, lower stress at break, σ_b, and slightly higher deformation at break, ε_b, than HG-AGMA1-20, given its lower cross-linking degree. Both composites were much tougher and stiffer than plain hydrogels, as revealed by the significantly higher σ_b, ε_b, and E values. On the whole, their mechanical behavior was dominated by the fibrous component, as it may be inferred by the similar mechanical performance to Fiber-PLLA, and in line with what was previously reported for other polyester-based hydrogel composites.[39] However, both Comp-10 and Comp-20 showed remarkably higher σ_b values than Fiber-PLLA, probably due to the efficient PLLA/hydrogel surface adhesion, deriving from the Michael reaction between primary amine groups on PLLA surface and the acrylamide groups of AGMA1 precursors.

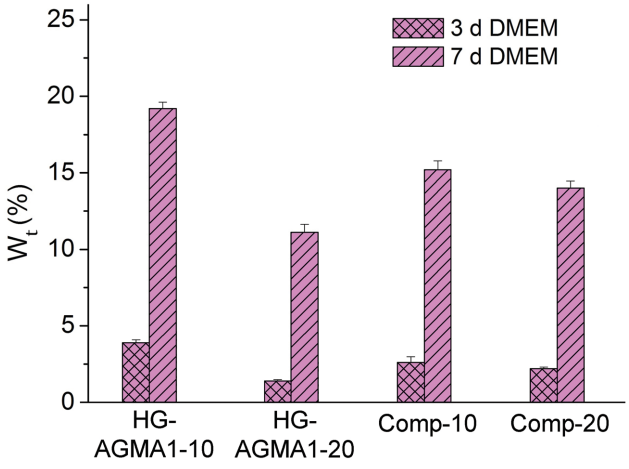

Figure 7. Weight loss after 3 and 7 d immersion in DMEM.

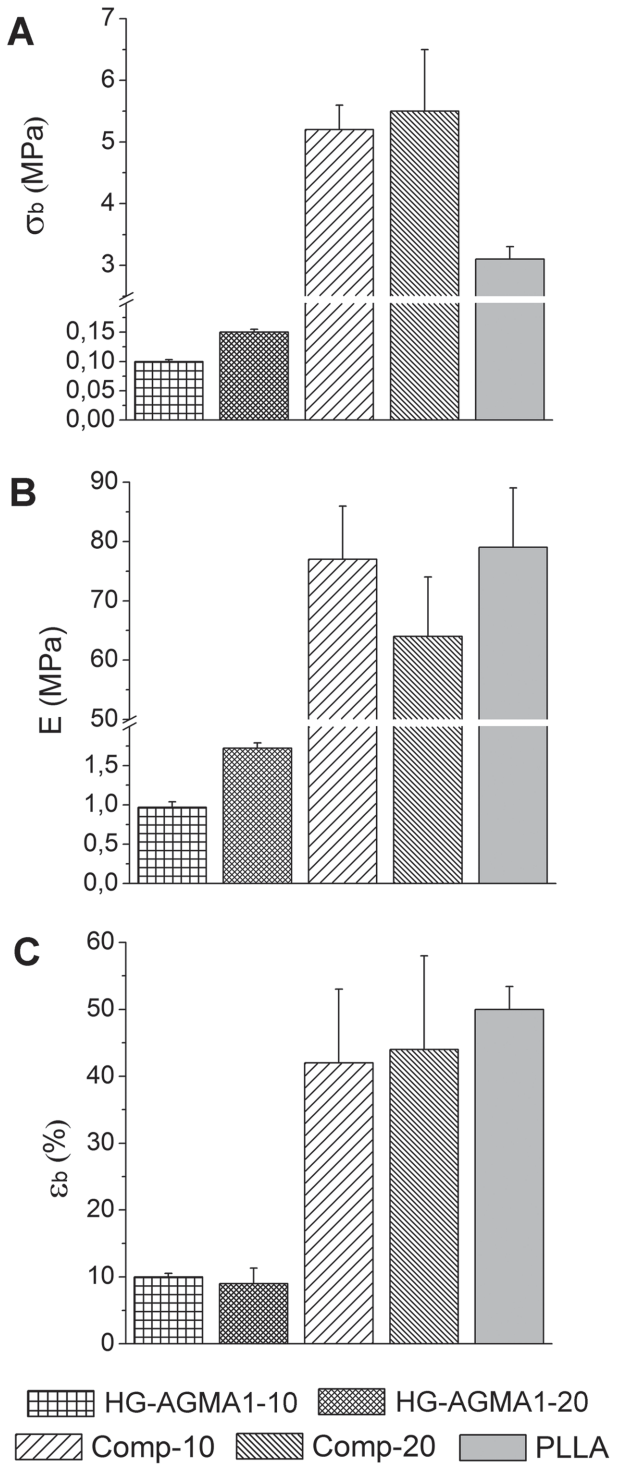

Figure 8. Tensile stress–strain mechanical data. A) Stress at break (σ_b). B) Elastic modulus. C) Deformation at break (ε_b).

3.6. In Vitro Studies with Human Pluripotent Stem Cells

Two hPSCs lines, namely hESCs and hiPSCs, were cultured on PLLA/AGMA1 composites to evaluate their ability to sustain stem cell adhesion and proliferation, and to maintain stemness. The ability of PLLA fibers to support stem cell adhesion, proliferation, as well as differentiation, had previously been extensively described.[40,41]

hiPSCs have been acknowledged as effective substitutes for hESCs and represent a promising alternative cell source for regenerative medicine. hESCs and hiPSCs share pluripotency, that is, the ability to differentiate into any specialized cell type, and self-renewal characteristic, that is, the ability to undergo numerous cycles of mitosis without altering the undifferentiated state. Maintenance of pluripotency and self-renewal ability of hPSCs represents a great potential for drug screening, disease modeling, and regenerative medicine.[42,43] Dysregulation of self-renewal capacity would reduce pluripotency. Normally, hPSCs are grown and maintained in the undifferentiated state on feeder layer cells or matrices, as for instance Matrigel, a complex mixture of extracellular matrix proteins, which can engage multiple cell surface targets involved in self-renewal mechanism.[41,44–47] hPSC technology requires definite, scalable, safe, and free of animal products culture conditions, and the development of culture systems for high quality expansion and differentiation of hPSCs is still a challenge. PLLA/AGMA1 composites hydrogels, thanks to the excellent mechanical properties and degradability, may represent good substrates for preserving hPSCs characteristics in feeder-free conditions, provided they exhibit the same good biocompatibility of their components. Cell viability tests showed that degradation products did not induce toxic effects on both hPSCs lines. After 24 h incubation in the presence of degradation products, the average hESCs viability was in the 90%–93% range, with no statistically significant difference in the cell viability ($p > 0.05$) between all types of scaffolds. Similar results were obtained in hiPSCs cultures.

In hPSCs culturing, cells were seeded onto PLLA/AGMA1 composites without treatment with conventional coatings. Cells plated on Matrigel-coated Tissue Culture Plates (TCPS-Mg) were used as positive control set as 100%. hPSCs were plated on each scaffold and their behavior was analyzed in terms of proliferation, morphology, and undifferentiated state (Figure 9).

hPSCs growth was determined after 1 and 7 d of culture using cells cultured on Matrigel-coated Tissue Culture Plates (TCPS-Mg) as positive control. The cell proliferation rate, defined as the increase in the ratio of cell number at days 1 and 7 over the seeded cell number, was determined (Figure 9A). At day 1, the fold increase value of both hPSCs on Matrigel was ≈1, that is, higher than hydrogels (0.3 for both hPSCs), composites (0.3 for hESCs and 0.4–0.6 for hiPSCs), and PLLA (nearly 0.3 for hESCs and 0.5 for hiPSCs) (Figure 9A), indicating some initially incomplete hPSCs adhesion to the substrates. At day 7, significantly increased cell proliferation was observed on PLLA (≈2 for hESCs and 2.5 for hiPSCs), on Comp-10 (1.5 for both hPSCs), and on Comp-20 (1 for hESCs and 2.3 for hiPSCs). The two cell lines behaved differently: hESCs showed a higher proliferation rate on Comp-10 than on Comp-20 ($^{*}p < 0.5$ on day 7); the reverse was true for hiPSCs ($^{***}p < 0.001$ on day 7). This fact suggested cell-line-specific effects, in line with previously observed differences in adhesive properties to different substrates.[44,32] All these results provided evidence that both PLLA/AGMA1 composites, but not plain hydrogels, warrant potential as binding sites for hPSCs.

The cell morphology of cultured hPSCs was examined by fluorescence microscopy. One day post plating, the majority of adherent hPSCs on TCPS-Mg were flattened, with a fibroblast-like morphology, and spread away from each other (Figure 9B), confirming previous observations.[32] Under the same culturing conditions, individual cells rather than colonies were observed on HG-AGMA1-10 and HG-AGMA1-20 (Figure 9B). By contrast, hPSCs plated on PLLA, Comp-10, and Comp-20 showed spherical morphology with minimal expansion of cytoplasm and formed compact separate colonies (Figure 9B). No further analysis was performed on hPSCs cultured on HG-AGMA1-10 and HG-AGMA1-20.

qRT-PCR and immunofluorescence analyses of self-renewal markers were carried out at day 7 on the cells cultured on PLLA, Comp-10, and Comp-20, to assess whether the growing cells expressed undifferentiated properties. In particular, qRT-PCR analyses were performed for OCT4, NANOG, and SOX2 genes, all involved in stem cell self-renewal (Figure 10A).[48]

Both hESCs and hiPSCs expressed all pluripotency factors analyzed. Interestingly, OCT4, NANOG, and SOX2 gene expression was significantly higher in hESCs cultured on Comp-20 ($^{***}p < 0.01$, $^{*}p < 0.01$, and $^{***}p < 0.001$, respectively) compared to TCPS-Matrigel control. Also hiPSCs cultured on Comp-10 and Comp-20 expressed higher levels of OCT4 when compared to TCPS-Matrigel control ($^{***}p < 0.001$), but as regards the other genes tested, the only significant difference detected was the NANOG expression between Comp-20- and TCPS-Matrigel cultures ($^{**}p < 0.01$).

Compared to PLLA cell cultures, hESCs grown on Comp-20 showed a greater OCT4, NANOG, and SOX2 expression ($^{***}p < 0.001$, $^{*}p < 0.01$, and $^{***}p < 0.001$, respectively), whereas only OCT4 was significantly higher in hiPSCs grown on Comp-20 ($^{***}p < 0.001$). For both cell lines, no statistically significant difference between Comp-10 and PLLA cultures on the expression of NANOG

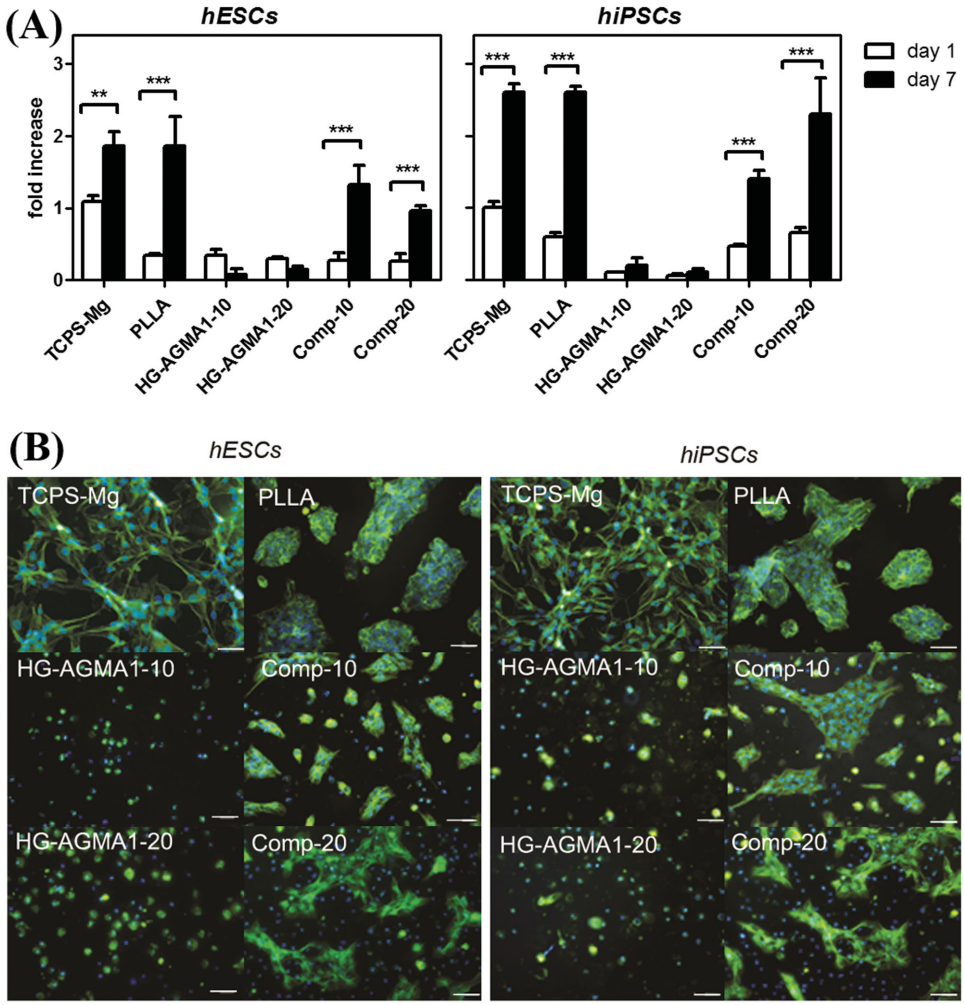

Figure 9. Proliferation and cell morphology analyses of hESCs and hiPSCs cultured on different substrates. A) Cell growth evaluation performed at days 1 and 7 of culture. Cell proliferation (fold increase) is plotted as the ratio between viable cells and initial seeded cell number (day 0). Statistical analysis was performed comparing day 7 versus day 1 values and normalized to the TCPS-Mg controls (***$p < 0.001$; **$p < 0.01$). B). Representative immunofluorescence images showing the localization of cytoskeletal β-tubulin (green) proteins in hESCs and hiPSCs cultured on different substrates at 24 h from cell seeding. Nuclei were counterstained with Hoechst 33342 (blue). Scale bar: 100 μm.

(#$p > 0.05$) and SOX2 (#$p > 0.05$) was observed. In the same tests, both cell lines cultured on PLLA and TCPS-matrigel gave quite similar results. All together, these results showed that the self-renewal of hESCs and hiPSCs was stably maintained on composites. This was further confirmed by the positive immunostaining of the stemness marker OCT4 (Figure 10B).

hPSCs adhered to both hydrogels and composites, but those cultured on plane hydrogels (bulk elastic moduli 1.0 and 1.3 MPa) did not form colonies. Conversely, hPSCs cultured on composites (bulk elastic moduli 80 and 65 MPa) showed adhesiveness, spreading, and proliferation into colonies, as well as stemness maintenance. From a general perspective, these results are in line with the reported stiffness-dependent adhesiveness and ability to support hESC colony formation reported for polyacrylamide-based hydrogels.[49] Besides bulk properties, the topographical features of the composite surfaces, characterized by a clearly visible PLLA texture under the hydrogel surface (Figure 3CD and Figure S4, Supporting Information), are expected to largely determine the stiffness locally perceived by cells and to play a relevant role in determining cell behavior.[50,51]

4. Conclusions

New bioactive composites based on PLLA and AGMA1, a biocompatible guanidine-substituted PAA whose repeating unit is reminiscent of the RGD motif, were obtained in five steps: preparing PLLA electrospun nanofiber mats; preparing α,ω-acrylamide-end-capped AGMA1 oligomers; surface-modifying the mats with nitrogen plasma; embedding the treated mats with 30% aqueous solutions of

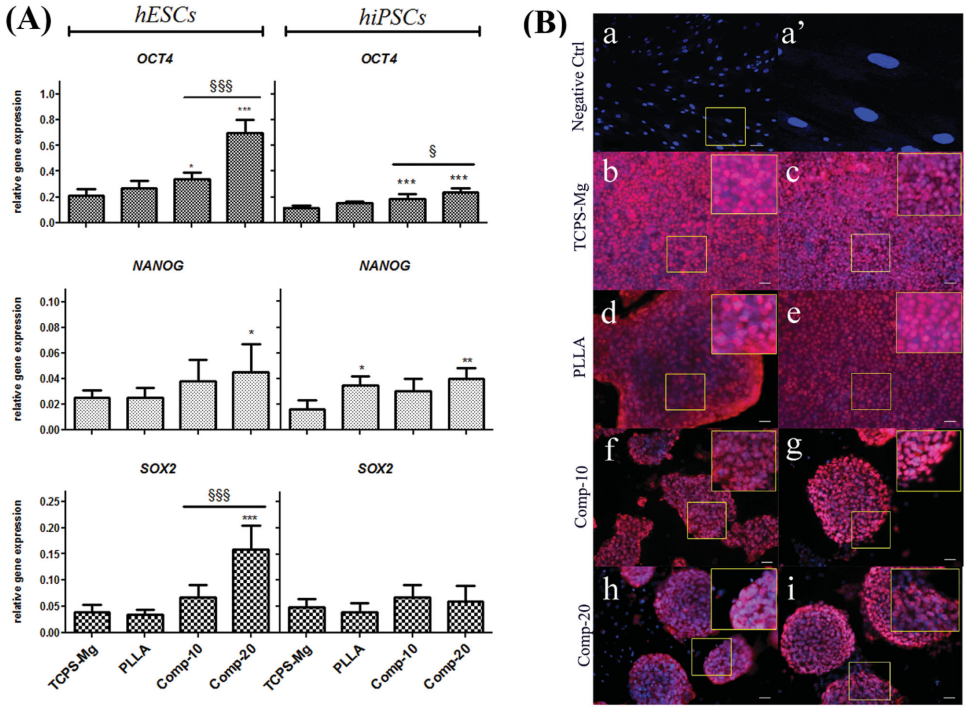

Figure 10. Pluripotency markers in hESCs and hiPCSs cultured for 7 d on different substrates. A) Quantitative RT-PCR analysis for pluripotent marker gene (OCT4, NANOG, SOX2) expression in both cell types. Statistical analysis was performed against TCPS-Mg (***$p < 0.001$; **$p < 0.01$) and between all scaffolds ($^{§§§}p < 0.001$). Data are the mean ± SD ($n = 3$). B) Representative images of immunofluorescence staining to detect OCT4 (red); nuclei were counterstained with Hoechst 33342 (blue). Human skin fibroblasts (HSFs) were used as negative controls for OCT4 (a, a′). Magnified areas of cells are shown in insets. Scale bars = 50 µm. Due to hydrogel degradation, gene expression analysis and immunofluorescence staining were not performed on HG-AGMA1-10 and HG-AGMA1-20 samples.

the oligomers doped with a little amount of 4,4′-azobis-(4-cyanovaleric) acid; curing by UV irradiation, which triggered the radical polymerization of the AGMA1 oligomers. The resultant composites absorbed large amounts of water forming reinforced hydrogels that effectively combined the biomimetic properties and softness of the surface-exposed AGMA1 hydrogel with the strength of PLLA mats. In the swollen state the composites were translucent, soft, and pliable, yet mechanically strong. They maintained their physical integrity on standing in water, since the hydrogel portion was covalently grafted to the PLLA nanofibers via the addition reaction of the surface amine groups, introduced on the fibers by treating with plasma nitrogen, to a part of the terminal acrylic double bonds of the parent AGMA1 oligomers.

Preliminary experiments showed that the PLLA-AGMA1 composites successfully support short-term self-renewal of hPSCs. Admittedly, more detailed and long-lasting experiments are needed to fully assess their potential for biomedical applications both in vitro, as scaffolds for long-term cell (including stem cell) culturing, and in vivo as implantable materials. However, the PLLA-AGMA1 composites, besides giving favorable preliminary results as substrates for hESCs and hiPSCs culturing, proved endowed with good mechanical properties, and their components are known to be biocompatible and biodegradable, albeit slowly as regards PLLA. On this basis, it may be reasonably concluded that they represent promising new entries in the biomaterial field.

Supporting Information

Supporting Information is available from the Wiley Online Library or from the author.

Acknowledgements: This work was supported by COST Action MP1206: "Electrospun nano-fibres for bio inspired composite materials and innovative industrial applications," by COST Action MP1101 "Biomedical applications of atmospheric pressure plasma technology." The MS laboratory was supported by EU-FP7 CARE-MI, FWO (G.0606.12, G.0A88.13). The authors thank Robin Duelen for his support in hPSCs cultures. Professor A. Pollicino is acknowledged for his support in XPS analysis.

Received: February 18, 2016; Revised: May 17, 2016; Published online: June 10, 2016; DOI: 10.1002/mabi.201600061

Keywords: atmospheric pressure nonequilibrium plasma; electrospun poly-L-lactic nanofibers; human pluripotent stem cells; polyamidoamines; poly-L-lactic acid-AGMA1 hydrogel composites

[1] N. A. Peppas, J. Z. Hilt, A. Khademhosseini, R. Langer, *Adv. Mater.* **2006**, *18*, 1345.
[2] A. Sivashanmugam, R. A. Kumar, M. V. Priya, S. V. Nair, R. Jayakumar*Eur. Polym. J.* **2015**, *72*, 543.
[3] E. Caló, V. V. Khutoryanskiy*Eur. Polym. J.* **2015**, *65*, 252.
[4] Q. V. Nguyen, D. P. Huynh, J. H. Park, D. S. Lee*Eur. Polym. J.* **2015**, *72*, 602.
[5] P. Ferruti, *J. Polym. Sci. A: Polym. Chem.* **2013**, *51*, 2319.
[6] P. Ferruti, S. Bianchi, E. Ranucci, F. Chiellini, A. M. Piras, *Biomacromolecules* **2005**, *6*, 2229.
[7] V. Magnaghi, V. Conte, P. Procacci, G. Pivato, P. Cortese, E. Cavalli, G. Pajardi, E. Ranucci, F. Fenili, A. Manfredi, P. Ferruti, *J. Biomed. Mater. Res. A* **2011**, *98*, 19.
[8] N. Mauro, A. Manfredi, E. Ranucci, P. Procacci, M. Laus, D. Antonioli, C. Mantovani, V. Magnaghi, P. Ferruti, *Macromol. Biosci.* **2013**, *13*, 332.
[9] E. Jacchetti, E. Emilitri, S. Rodighiero, M. Indrieri, A. Gianfelice, C. Lenardi, A. Podestà, E. Ranucci, P. Ferruti, P. Milani, *J. Nanobiotechnol.* **2008**, *6*, 14.
[10] G. Dos Reis, F. Fenili, A. Gianfelice, G. Bongiorno, D. Marchesi, P. E. Scopelliti, A. Borgonovo, A. Podestà, M. Indrieri, E. Ranucci, P. Ferruti, C. Lenardi, P. Milani, *Macromol. Biosci.* **2010**, *10*, 842.
[11] N. Mauro, F. Chiellini, C. Bartoli, M. Gazzarri, M. Laus, D. Antonioli, P. Griffiths, A. Manfredi, E. Ranucci, P. Ferruti, *J. Tissue Eng. Regen. Med.* **2016**, DOI: 10.1002/term.2115.
[12] K. Tanahashi, S. Jo, A. G. Mikos*Biomacromolecules* **2002**, *3*, 1030.
[13] J. Franchini, E. Ranucci, P. Ferruti, M. Rossi, R. Cavalli, *Biomacromolecules* **2006**, *7*, 1215.
[14] R. Cavalli, A. Bisazza, R. Sessa, P. Luca, F. Fenili, A. Manfredi, E. Ranucci, P. Ferruti, *Biomacromolecules* **2010**, *11*, 2667.
[15] N. Tonna, F. Bianco, M. Matteoli, C. Cagnoli, F. Antonucci, A. Manfredi, N. Mauro, E. Ranucci, P. Ferruti, *Sci. Technol. Adv. Mater.* **2014**, *15*, 045007.
[16] F. Martello, A. Tocchio, M. Tamplenizza, I. Gerges, V. Pistis, R. Recenti, M. Bortolin, M. Del Fabbro, S. Argentiere, P. Milani, C. Lenardi, *Acta Biomater.* **2014**, *10*, 1206.
[17] I. Gerges, M. Tamplenizza, E. Rossi, A. Tocchio, F. Martello, C. Recordati, D. Kumar, N. R. Forsyth, Y. Liu, C. Lenardi, *Macromol. Biosci.* **2016**, *6*, mabi.201500386.
[18] L. A. Bosworth, L.-A. Turner, S. H. Cartmell, *Nanomed. Nanotechnol. Biol. Med.* **2013**, *9*, 322.
[19] W. Zhao, Z. Shi, X. Chen, G. Yang, C. Lenardi, C. Liu, *Composites Part B* **2015**, *76*, 292.
[20] S. Xu, L. Deng, J. Zhang, L. Yin, A. Dong, *J. Biomed. Mater. Res. Part B* **2016**, *104B*, 640.
[21] S. Lin, C. Cao, Q. Wang, M. Gonzalez, J. E. Dolbow, X. Zhao, *Soft Matter* **2014**, *10*, 7519.
[22] J. Jang, H. Oh, J. Lee, T.-H. Song, Y. H. Jeong, D.-W. Cho, *Appl. Phys. Lett.* **2013**, *102*, 211914.
[23] A. G. Mikos, A. J. Thorsen, L. A. Czerwonka, Y. Bao, R. Langer, *Polymer* **1994**, *35*, 1068.
[24] P. X. Ma, R. Y. Zhang, *J. Biomed. Mater. Res.* **1999**, *46*, 60.
[25] H. Lo, S. Kadiyala, S. E. Guggino, K. W. Leong, *J. Biomed. Mater. Res.* **1996**, *30*, 475.
[26] E. Saino, M. L. Focarete, C. Gualandi, E. Emanuele, A. I. Cornaglia, M. Imbriani, L. Visai, *Biomacromolecules* **2011**, *12*, 1900.
[27] A. Higuchi, S.-H. Kao, Q.-D. Ling, Y.-M. Chen, H.-F. Li, A. A. Alarfaj, M. A. Munusamy, K. Murugan, S.-C. Chang, H.-C. Lee, S.-T. Hsu, S. S. Kumar, A. Umezawa, *Sci. Rep.* **2015**, *5*, 18136.
[28] C. McKee, M. Perez-Cruet, F. Chavez, G. R. Chaudhry, *World J. Stem Cells* **2015**, *7*, 1064.
[29] C. Lee-Thedieck, J. P. Spatz, *Macromol. Rapid Commun.* **2012**, *33*, 1432.
[30] G. Beamson, D. Briggs, *High Resolution XPS of Organic Polymers: the Scienta ESCA300 Database*, Wiley Interscience, New York **1992**.
[31] T. E. Ludwig, M. E. Levenstein, J. M. Jones, W. T. Berggren, E. R. Mitchen, J. L. Frane, L. J. Crandall, C. A. Daigh, K. R. Conrad, M. S. Piekarczyk, R. A. Llanas, J. A. Thomson, *Nat. Biotechnol.* **2006**, *24*, 185.
[32] D. Bae, S.-H Moon, B. G. Park, S.-J Park, T. Jung, J. S. Kim, K. B. Lee, H. M. Chung, *Biomaterials* **2014**, *35*, 916.
[33] K. Gauthaman, J. R. Venugopal, F. C. Yee, G. S. L. Peh, S. Ramakrishna, A. Bongso, *J. Cell Mol. Med.* **2009**, *13*, 3475.
[34] C. Gualandi, C.-D. Vo, M. L. Focarete, M. Scandola, A. Pollicino, G. Di Silvestro, N. Tirelli, *Macromol. Rapid Commun.* **2013**, *34*, 51.
[35] D. Han, A. J. Steckl, *Langmuir* **2009**, *25*, 9454.
[36] C. Gualandi, M. Govoni, L. Foroni, S. Valente, M. Bianchi, E. Giordano, G. Pasquinelli, F. Biscarini, M. L. Focarete, *Eur. Polym. J.* **2012**, *48*, 2008.
[37] L. S. Dolci, S. D. Quiroga, M. Gherardi, R. Laurita, A. Liguori, P. Sanibondi, A. Fiorani, L. Calzà, V. Colombo, M. L. Focarete, *Plasma Processes Polym.* **2014**, *11*, 203.
[38] S. Zanini, C. Riccardi, A. Natalello, G. Cappelletti, D. Cartelli, F. Fenili, A. Manfredi, E. Ranucci, *Mater. Res. Express* **2014**, *1*, 035001.
[39] D. G. T Strange, K. Tonsomboon, M. L. Oyen, *J. Mater. Sci. Mater. Med.* **2014**, *25*, 681.
[40] R. J. McMurray, N. Gadegaard, P. M. Tsimbouri, K. V. Burgess, L. E. McNamara, R. Tare, K. Murawski, E. Kingham, R. O. C. Oreffo, M. J. Dalby, *Nat. Mater.* **2011**, *10*, 637.
[41] E. Kingham, K. White, N. Gadegaard, M. J. Dalby, R. O. C. Oreffo, *Small* **2013**, *9*, 2140.
[42] J. A. Thomson, J. Itskovitz-Eldor, S. S. Shapiro, M. A. Waknitz, J. J. Swiergiel, V. S. Marshall, J. M. Jones, *Science* **1998**, *282*, 1145.
[43] K. Takahashi, K. Tanabe, M. Ohnuki, M. Narita, T. Ichisaka, K. Tomoda, S. Yamanaka, *Cell* **2007**, *131*, 861.
[44] A. Singh, S. Suri, T. Lee, J. M. Chilton, M. T. Cooke, W. Chen, J. Fu, S. L. Stice, H. Lu, T. C. McDevitt, A. J. García, *Nat. Methods* **2013**, *10*, 438.
[45] T. Miyazaki, S. Futaki, H. Suemori, Y. Taniguchi, M. Yamada, M. Kawasaki, M. Hayashi, H., N. Nakatsuji , K. Sekiguchi, E. Kawase, *Nat. Commun.* **2012**, *3*, 1236.
[46] H. K. Kleinman, G. Martin, *Semin. Cancer Biol.* **2005**, *15*, 378.
[47] M. T. Lam, M. T. Longaker, *J. Tissue Eng. Regen. Med.* **2012**, *6*, s80.
[48] J. L. Chew, Y. H. Loh, W. Zhang, X. Chen, W. L. Tam, L. S. Yeap, P. Li, Y. S. Ang, B. Lim, P. Robson, H. H. Ng, *Mol. Cell Biol.* **2005**, *25*, 6031.
[49] S. Musah, S. A. Morin, P. J. Wrighton, D. B. Zwick, S. Jin, L. L. Kiessling, *ACS Nano* **2012**, *6*, 10168.
[50] J. Y. Lim, H. J. Donahue, *Tissue Eng.* **2007**, *13*, 1879.
[51] S. Mitragotri, J. Lahann, *Nat. Mater.* **2009**, *8*, 15.